ACADEMIC PRESS

Available online at www.sciencedirect.com

SCIENCE DIRECT®

Journal of Computational Physics 185 (2003) 50–60

JOURNAL OF COMPUTATIONAL PHYSICS

www.elsevier.com/locate/jcp

Radiative transfer computations for optical beams

Arnold D. Kim[a,*,1], Miguel Moscoso[b,2]

[a] *Department of Mathematics, Stanford University, Stanford, CA 94305-2125, USA*
[b] *Departamento de Matemáticas, Escuela Politécnica Superior, Universidad Carlos III de Madrid, Avda. de la Universidad 30, 28911 Leganés, Spain*

Received 5 January 2002; received in revised form 23 July 2002; accepted 12 September 2002

Abstract

In this paper, we present a method for computing direct numerical simulations of narrow optical beam waves propagating and scattering in a plane-parallel medium. For these computations, we use Fourier and Chebyshev spectral methods for three-dimensional radiative transfer that also includes polar and azimuthal angle dependences. We treat anisotropic scattering with peaked forward scattering by using a Clenshaw–Curtis quadrature rule for the polar angle and an extended trapezoid rule for the azimuthal angle. To verify our results, we compare this spectral method to Monte Carlo simulations.

Keywords: Radiative transfer; Spectral methods; Beams; Anisotropic scattering

1. Introduction

The theory of radiative transfer models light propagation and scattering in random media [1,2]. Although this theory is well known, analytical solutions are not available except for relatively simple problems. Therefore, many have put forth a great deal of effort into developing numerical methods that accurately approximate solutions. For example, the searchlight problem in which a narrow beam impinges a scattering medium still represents a numerical challenge today.

Other than Monte Carlo simulations, there are few highly accurate methods that adequately compute solutions to this problem. We mention here the work of Chang and Ishimaru [3], Ganapol et al. [4], and Barichello and Siewert [5] among others. In these works, Fourier transform procedures are used for the transverse spatial variables leading to one-dimensional radiative transfer equations for each spatial frequency. They all consider normally incident beams to take the advantage of the cylindrical symmetry that

* Corresponding author. Tel.: 1-650-723-2975; fax: 1-650-725-4066.
E-mail addresses: adkim@math.stanford.edu (A.D. Kim), moscoso@math.uc3m.es (M. Moscoso).
[1] Supported by the National Science Foundation (Grant No. DMS-0071578).
[2] Supported by DGES Grant PB98-0142-C04-01 from the Autonomous Region of Madrid (Strategic Groups Action) and by Grant RTN2-2001-00349 from the European Union.

0021-9991/02/$ - see front matter
PII: S0021-9991(02)00047-5

reduces the dimension of the problem from five independent variables to four. Chang and Ishimaru solve these resultant equations using a two-dimensional Gaussian quadrature rule and an eigenvalue–eigenvector technique. Ganapol et al., and Barichello and Siewert consider the additional assumption of isotropic scattering. Then the solution to the searchlight problem can be found through solving the so-called *pseudo-problem* which is a modified, one-dimensional equation of transfer [6].

In this paper, we undertake the searchlight problem. This particular problem is especially relevant to studies of spatially narrow optical beams propagating in scattering media such as fog, clouds as well as biological tissue [2]. In these applications the scattering is usually anisotropic with highly peaked forward scattering phase functions. Here we take special consideration to develop direct numerical simulation methods that do not rely too heavily on any particular aspects of this problem. In particular, neither normally incident beams nor isotropic scattering is assumed. We consider the problem presented here as an initial effort toward effectively addressing large scale radiative transfer computations, such as problems with time, polarization, and inhomogeneities.

Three numerical treatments comprise the numerical method in total. As in the previous works we use Fourier transforms for the transverse spatial variables. We use a Chebyshev spectral method for the vertical spatial variable. Chebyshev spectral methods have already demonstrated extremely accurate results with super-algebraic convergence rates for one-dimensional problems [7]. This spectral approximation produces a sparse system of integral equations for the angle dependent expansion coefficients. This system of integral equations is solved using Nyström methods that use the Clenshaw–Curtis rule for the polar angle variable and the extended trapezoid rule for the azimuthal angle variable.

After presenting the radiative transfer equation and boundary conditions for our model problem in Section 2, we briefly explain the spectral method for this problem in Section 3 by identifying its three key features. In Section 4, we present some example computations in which we compare results from the spectral code with Monte Carlo simulations to ensure consistent results. We conclude in Section 5 with some final remarks.

2. The radiative transfer equation

The radiative transfer equation

$$\widehat{\Omega}\cdot\nabla I(\mathbf{r},\widehat{\Omega})+\sigma_{\mathrm{a}}(\mathbf{r})I(\mathbf{r},\widehat{\Omega})=-\sigma_{\mathrm{s}}(\mathbf{r})\left[I(\mathbf{r},\widehat{\Omega})-\int_{\mathbb{S}^2}P(\widehat{\Omega},\widehat{\Omega}')I(\mathbf{r},\widehat{\Omega}')\,\mathrm{d}\widehat{\Omega}'\right] \tag{1}$$

models continuous light propagation in a scattering and absorbing media [1,2]. The fundamental quantity of radiative transfer is the specific intensity or radiance I. It depends on a position vector $\mathbf{r}$ and a unit direction vector $\widehat{\Omega}$. The scattering cross-section σ_{s} and the absorption cross-section σ_{a} characterize the optical properties of the medium. The integral operation in (1) that involves the scattering phase function $P(\widehat{\Omega},\widehat{\Omega}')$ takes place over the unit sphere $\mathbb{S}^2$. This phase function dictates the directional distribution of light that scatters in direction $\widehat{\Omega}$ due to waves of unit energy density incident in direction $\widehat{\Omega}'$, and it is normalized according to

$$\int_{\mathbb{S}^2}P(\widehat{\Omega},\widehat{\Omega}')\,\mathrm{d}\widehat{\Omega}'=1. \tag{2}$$

Consequently, when $\sigma_{\mathrm{a}}=0$ Eq. (1) is a statement of power conservation. In (1) we have neglected polarization effects.

For this study, we are interested in computing solutions to Eq. (1) in a homogeneous plane-parallel medium on which a collimated beam is incident in some specific direction. Because the medium is

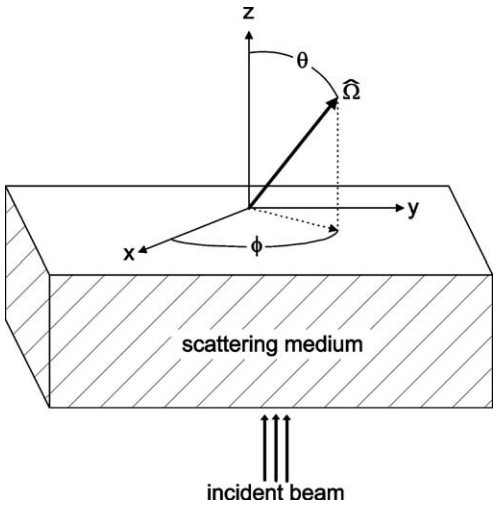

Fig. 1. A sketch of the plane-parallel problem.

homogeneous, the scattering and absorption cross-sections are constant. Representing (1) in Cartesian coordinates (see Fig. 1), we have

$$\left[\mu\frac{\partial}{\partial z}+\sqrt{1-\mu^2}\left(\cos\phi\frac{\partial}{\partial x}+\sin\phi\frac{\partial}{\partial y}\right)+\sigma_t\right]I(x,y,z,\mu,\phi)$$
$$=\sigma_s\int_0^{2\pi}\int_{-1}^{+1}P(\mu,\phi,\mu',\phi')I(x,y,z,\mu',\phi')\,d\mu'\,d\phi', \tag{3}$$

where $\sigma_t=\sigma_s+\sigma_a$. We define the plane-parallel medium as $0<z<L$ where the x and y variables are unbounded ($-\infty<x,y<\infty$). We define the cosine of the polar angle as $\mu=\cos\theta$ which ranges from $-1\leqslant\mu\leqslant 1$ and the azimuthal angle as ϕ which ranges from $0\leqslant\phi<2\pi$.

For our discussion here, we assume that the boundaries are index-matched. In other words, the refractive index in the medium contained between the two boundary planes $0<z<L$ is the same as the refractive index outside of the medium $z<0$ and $z>L$. At $z=0$, we consider a collimated beam of width w_0 incident in some specified direction (μ_0,ϕ_0). This beam, incorporated into the mathematical problem through the boundary condition

$$I(x,y,z=0,\mu,\phi)=F_0\exp\left[-\frac{(x^2+y^2)}{w_0^2}\right]\delta(\mu-\mu_0)\delta(\phi-\phi_0) \tag{4}$$

for $0<\mu\leqslant 1$ and $0\leqslant\phi<2\pi$, is the only source of radiation. Hence, at $z=L$, we impose that no light enters into the medium through the boundary condition

$$I(x,y,z=L,\mu,\phi)=0 \tag{5}$$

for $-1\leqslant\mu<0$ and $0\leqslant\phi<2\pi$. Finally, we impose that the specific intensity vanishes sufficiently fast as the distance from the beam center ($x=y=0$) increases

$$I(x,y,z,\mu,\phi)\to 0\quad\text{as } x^2+y^2\to\infty. \tag{6}$$

We note that an alternative way of describing beam sources at the boundary is to solve only for the diffuse component of the intensity. In that case one obtains a homogeneous boundary condition instead of (4), but (3) has an additional source term $F(x,y,z,\mu,\phi)$ [3].

3. Numerical scheme for radiative transfer

Three numerical treatments comprise the numerical scheme in total. First, we treat the transverse spatial variables x and y using Fourier spectral methods. Then, we approximate the z-dependence of the specific intensity by a Chebyshev spectral method to obtain a linear system of integral equations. Finally, we numerically solve this system using a Nyström method that uses the Clenshaw–Curtis quadrature rule for the polar angle and an extended trapezoid rule for the azimuthal angle.

3.1. Fourier spectral method

Because of the condition given in Eq. (6), we are motivated to consider the Fourier transform

$$\hat{I}(\xi,\eta,z,\mu,\phi)=\int_{-\infty}^{+\infty}\int_{-\infty}^{+\infty} I(x,y,z,\mu,\phi)\exp[-\mathrm{i}\xi x-\mathrm{i}\eta y]\,\mathrm{d}x\,\mathrm{d}y \tag{7}$$

of the specific intensity I with respect to x and y. The Fourier transform of the radiative transfer equation that governs $\hat{I}$ is then

$$\left[\mu\frac{\partial}{\partial z}+\mathrm{i}\sqrt{1-\mu^2}(\xi\cos\phi+\eta\sin\phi)+\sigma_{\mathrm{t}}\right]\hat{I}(\xi,\eta,z,\mu,\phi)$$
$$=\sigma_{\mathrm{s}}\int_0^{2\pi}\int_{-1}^{+1} P(\mu,\phi,\mu',\phi')\hat{I}(\xi,\eta,z,\mu',\phi')\,\mathrm{d}\mu'\,\mathrm{d}\phi'. \tag{8}$$

The boundary condition (4) transforms to

$$\hat{I}(\xi,\eta,z=0,\mu,\phi)=F_0\pi w_0^2\exp\left[-\frac{1}{4}w_0^2(\xi^2+\eta^2)\right]\delta(\mu-\mu_0)\delta(\phi-\phi_0) \tag{9}$$

for $0<\mu\leqslant 1$ and $0\leqslant\phi<2\pi$. The boundary condition (5) transforms to

$$\hat{I}(\xi,\eta,z=L,\mu,\phi)=0 \tag{10}$$

for $-1\leqslant\mu<0$ and $0\leqslant\phi<2\pi$. Notice that the dependence on (ξ,η) in (8)–(10) is parametric and so one can numerically solve for each spatial frequency pair needed in a two-dimensional discrete Fourier transform since they are decoupled from all other frequency pairs. In addition, because the intensity is a real-valued function, one only needs "half" of the two-dimensional spatial frequency spectrum to invert numerically the specific intensity into the physical domain. We also note that if $\mu_0=1$ then the problem has cylindrical symmetry and the transfer equation (8) and the boundary conditions (9) and (10) depend only on $v=(\xi^2+\eta^2)^{1/2}$.

3.2. Chebyshev spectral method

Since the specific intensity's dependence on (ξ,η) is parametric in (8), we suppress this dependence in the notation that follows. First, we perform the change variables $s=2z/L-1$ in (8) and obtain

$$\frac{2\mu}{L}\frac{\partial\hat{I}(s,\mu,\phi)}{\partial s}+\gamma(\mu,\phi)\hat{I}(s,\mu,\phi)=\sigma_{\mathrm{s}}\int_0^{2\pi}\int_{-1}^{+1} P(\mu,\phi,\mu',\phi')\hat{I}(s,\mu',\phi')\,\mathrm{d}\mu'\,\mathrm{d}\phi', \tag{11}$$

where

$$\gamma(\mu,\phi)=\sigma_{\mathrm{t}}+\mathrm{i}\sqrt{1-\mu^2}(\xi\cos\phi+\eta\sin\phi). \tag{12}$$

The spatial domain of this problem is $-1 < s < 1$. Next, we approximate the s-dependence of the specific intensity with a Chebyshev spectral approximation

$$\hat{I}(s,\mu,\phi) \cong \sum_{k=0}^{N} a_k(\mu,\phi) T_k(s), \tag{13}$$

where $T_k(s) = \cos[k\cos^{-1}(s)]$ is the Chebyshev polynomial of order k. The Chebyshev polynomials are normalized so that $T_k(\pm 1) = (\pm 1)^k$ and satisfy the orthogonality condition

$$\int_{-1}^{1} T_j(s) T_k(s) \frac{\mathrm{d}s}{\sqrt{1-s^2}} = \frac{\pi}{2} c_k \delta_{j,k}, \tag{14}$$

where $\delta_{j,k}$ is the Kronecker delta and

$$c_k = \begin{cases} 2 & \text{for } k = 0, N, \\ 1 & \text{for } k = 1, \ldots, N-1. \end{cases} \tag{15}$$

The spatial derivative of the specific intensity is given by another Chebyshev spectral approximation

$$\frac{\partial \hat{I}(s,\mu,\phi)}{\partial s} \cong \sum_{k=0}^{N} A_k(\mu,\phi) T_k(s), \tag{16}$$

where $A_k(\mu,\phi)$ is related to $a_k(\mu,\phi)$ through

$$a_k(\mu,\phi) = \frac{1}{2k}\left[c_{k-1} A_{k-1}(\mu,\phi) - A_{k+1}(\mu,\phi)\right] \quad \text{for } k = 1, 2, \ldots, N. \tag{17}$$

By substituting Eqs. (13) and (16) into (11) and using the orthogonality property (14), we obtain

$$\frac{2\mu}{L} A_k(\mu,\phi) + \gamma(\mu,\phi) a_k(\mu,\phi) = \sigma_s \int_0^{2\pi} \int_{-1}^{+1} P(\mu,\phi,\mu',\phi') a_k(\mu',\phi')\, \mathrm{d}\mu'\, \mathrm{d}\phi' \tag{18}$$

for $k = 0, \ldots, N$. Now, by applying (17) to (18), we obtain the linear system of integral equations:

$$\frac{2\mu}{L} A_0(\mu,\phi) + Q[a_0](\mu,\phi) = 0, \tag{19a}$$

$$\frac{2\mu}{L} A_1(\mu,\phi) + Q[A_0](\mu,\phi) - \frac{1}{2} Q[A_2](\mu,\phi) = 0, \tag{19b}$$

$$\frac{2\mu}{L} A_k(\mu,\phi) + \frac{1}{2k}\left[Q[A_{k-1}](\mu,\phi) - Q[A_{k+1}](\mu,\phi)\right] = 0 \quad \text{for } k = 2, \ldots, N-1, \tag{19c}$$

$$\frac{2\mu}{L} A_N(\mu,\phi) + \frac{1}{2N} Q[A_{N-1}](\mu,\phi) = 0, \tag{19d}$$

where

$$Q[f](\mu,\phi) = \gamma(\mu,\phi) f(\mu,\phi) - \sigma_s \int_0^{2\pi} \int_{-1}^{+1} P(\mu,\phi,\mu',\phi') f(\mu',\phi')\, \mathrm{d}\mu'\, \mathrm{d}\phi'. \tag{20}$$

This tridiagonal linear system of integral equations gives $N+1$ equations for $N+2$ unknown functions a_0, $A_0, A_1, \ldots, A_N$.

By adding an equation corresponding to the boundary conditions (9) and (10), one obtains a well-posed linear system of integral equations. At the boundary $s = -1$ ($z = 0$) we have the condition

$$\hat{I}(s=-1,\mu,\phi) = F_0\pi w_0^2 \exp\left[-\frac{1}{4}w_0^2(\xi^2+\eta^2)\right]\delta(\mu-\mu_0)\delta(\phi-\phi_0) = \sum_{k=0}^{N}(-1)^k a_k(\mu,\phi) \tag{21}$$

defined over the angular domain $0 < \mu \leqslant 1$ and $0 \leqslant \phi < 2\pi$. At the boundary located at $s = 1$ ($z = L$) we have the condition that

$$\hat{I}(s=+1,\mu,\phi) = 0 = \sum_{k=0}^{N} a_k(\mu,\phi) \tag{22}$$

defined over the angular domain $-1 \leqslant \mu < 0$ and $0 \leqslant \phi < 2\pi$. Hence, the composition of (21) and (22) yields a single equation over the entire unit sphere $\mathbb{S}^2$. Furthermore, by applying (17) to (21) and (22), we obtain the remaining equation needed in terms of the unknown functions given in (19a)–(19d).

We mention here that in solving the transfer equation, one often splits its solution into the ballistic (uncollided) component and the diffuse (collided) component. The ballistic component has a trivial singular solution given by geometric optics. The diffuse component arises from one or more scattering processes and satisfies the radiative transfer equation (3) with the additional source term

$$\hat{F}(s,\mu,\phi) = \sigma_s F_0 \pi w_0^2 P(\mu,\phi,\mu_0,\phi_0)\exp\left[-\frac{w_0^2}{4}(\xi^2+\eta^2) - \gamma(\mu_0,\phi_0)\frac{L(s+1)}{2\mu_0}\right] \tag{23}$$

and homogeneous boundary conditions. This source contains oscillating terms proportional to $\exp[-\mathrm{i}\xi Ls]$ and $\exp[-\mathrm{i}\eta Ls]$. For large values of ξL and ηL, this source oscillates rapidly in s thereby requiring spectral approximations of very high order. Hence, for a fixed number of Chebyshev modes, one is limited by medium thickness or transverse spatial resolution. However, by using the method we explain above, we do not encounter these oscillations explicitly. This particular approach is an important difference from those presented in [3,7,8].

3.3. Nyström method

Since spatial variables are treated with highly accurate spectral approximations, one can choose any suitable method to solve the system given by (19a)–(19d), (21), and (22). Here, we use a Nyström method [10] in which one chooses quadrature rules with particular abscissas and weights to approximate the integral operations. We choose this method solely because of its ease of implementation with good accuracy. For more detailed studies of scattering, a different numerical treatment may give better results and does not compromise any other aspect of the method. However, that decision is case dependent.

To compute approximations to the azimuthal integral operation, we use an extended trapezoid rule since functions of the azimuthal angle variable ϕ are 2π-periodic. This extended trapezoid rule takes the form

$$\int_0^{2\pi} f(\phi)\,\mathrm{d}\phi \cong \sum_{m=1}^{N_\phi} f(\phi_m) W_m^{(\phi)}. \tag{24}$$

The corresponding quadrature abscissas and weights are

$$\phi_m = \frac{2\pi(m-1)}{N_\phi}, \tag{25a}$$

$$W_m^{(\phi)} = \frac{2\pi}{N_\phi} \tag{25b}$$

for $m = 1, 2, \ldots, N_\phi$.

For the polar angle variable μ, we use a Clenshaw–Curtis quadrature rule. This is a closed Gaussian quadrature rule similar to a Chebyshev quadrature rule, but with a unit weight function [10]. This quadrature rule takes the form

$$\int_{-1}^{+1} f(\mu)\,\mathrm{d}\mu \cong \sum_{l=0}^{N_\mu}{}'' f(\mu_l) W_l^{(\mu)}, \tag{26}$$

where the double quotation marks on the summation indicate that the first and last terms are multiplied by a factor of 1/2. The quadrature abscissas and weights are defined as [10]

$$\mu_l = \cos\left(\frac{\pi l}{N_\mu}\right), \tag{27a}$$

$$W_l^{(\mu)} = \frac{4}{N_\mu} \sum_{\substack{n=0 \\ n\ \text{even}}}^{N_\mu}{}'' \frac{1}{1-n^2} \cos\left(n\frac{l\pi}{N_\mu}\right) \tag{27b}$$

for $l = 0, 1, \ldots, N_\mu$. Our numerical approximation to Q therefore takes the form

$$Q[f](\mu,\phi) \cong \gamma(\mu,\phi) f(\mu,\phi) - \sigma_s \sum_{l=0}^{N_\mu}{}'' W_l^{(\mu)} \sum_{m=1}^{N_\phi} P(\mu,\phi,\mu_l,\phi_m) f(\mu_l,\phi_m) W_m^{(\phi)}. \tag{28}$$

The boundary condition (21) contains delta functions in μ and ϕ. Here, we consider the case in which the angle of incidence corresponds to the quadrature abscissas $(\mu_0,\phi_0) = (\mu_{l'},\phi_{m'})$. Then we impose that

$$\sum_{k=0}^{N} (-1)^k a_k(\mu_l,\phi_m) \cong F_0 \pi w_0^2 \frac{\exp\left[-w_0^2(\xi^2+\eta^2)/4\right]}{W_{l'}^{(\mu)} W_{m'}^{(\phi)}} \delta_{l,l'} \delta_{m,m'}. \tag{29}$$

By considering the values of the Chebyshev expansion coefficients in (19a)–(19d), (21), and (22) only at the quadrature points, one obtains a bordered, block tridiagonal linear system of equations. Each of the $N+2$ blocks has size $q = N_\mu \times N_\phi$. A remarkable aspect of this system is that only the matrix approximating Q given by (28) and a q-vector with entries $2\mu_l/L$ are needed to store the entire bordered, block tridiagonal matrix (see [8] for details). Kim and Ishimaru [7] explain the application of the generalized deflated block elimination method [11] to solve this particular linear system efficiently.

3.4. Performance

The most intensive computation in this procedure is solving (19a)–(19d), (21), and (22) after implementing (28). This method requires $\mathrm{O}(q^3[N-1])$ operations where N is the number of Chebyshev modes and q is related to the number of quadrature points. Hence, the work scales linearly with respect to the number of Chebyshev modes, but cubically with respect to the number of quadrature abscissas. For example, a single linear system solve using $q = 80$ ($N_\mu = 10$ and $N_\phi = 8$) and $N = 33$ takes less than 2 s on a 850 MHz Pentium-III Linux workstation.

Although the accuracy and stability of this method is not restricted to isotropic scattering, highly anisotropic scattering requires several more quadrature abscissas to resolve sharp peaks in the phase function. Hence, computations using the Nyström method discussed above can become restrictively large because q increases. For this situation it is advantageous to consider alternate numerical methods to approximate the scattering operator that yield a smaller matrix approximating Q.

This linear system must be solved for each Fourier pair (ξ, η) in the computational spectrum. The work needed for the entire spectrum scales linearly with the number of spatial modes. However, a highly resolved transverse spatial computation requires solving several linear systems leading to large computations. In special situations such as cylindrical symmetry for normally incident beams, one can reduce the number for spatial modes needed by identifying additional symmetries in ξ and η. However, in general, these symmetries are not available.

4. Numerical examples

Here, we present computations for different values of the parameters of the problem. In addition, we examine the consistency of our numerical method by comparing it with Monte Carlo simulations. For our study we consider the Henyey–Greenstein phase function that is commonly used in studies of optics in fog, clouds, and biological tissue [2]. The Henyey–Greenstein phase function is defined as

$$P(\mu, \phi, \mu', \phi') = \frac{1}{4\pi} \frac{1 - g^2}{(1 + g^2 - 2g\cos\Theta)^{3/2}}, \tag{30}$$

where

$$\cos\Theta = \mu\mu' + \sqrt{(1-\mu^2)(1-\mu'^2)}\cos(\phi - \phi') \tag{31}$$

is the cosine of the scattering angle made between unit vectors (μ, ϕ) and (μ', ϕ'). This particular phase function is parameterized only by the anisotropy factor g and varies smoothly from isotropic scattering ($g = 0$) to narrow forward peak scattering ($g \sim 1$) or backward peak scattering ($g \sim -1$).

After computing the solution to the linear system for the Chebyshev expansion coefficients for each spatial frequency pair over some two-dimensional discrete spectrum, we invert that data into the physical domain using discrete Fourier transforms. To examine the data we compute the magnitude of the transmitted flux

$$F_{\mathrm{t}}(x, y) = \int_0^{2\pi} \int_0^{+1} \mu I(x, y, s = +1, \mu, \phi)\, \mathrm{d}\mu\, \mathrm{d}\phi \tag{32}$$

and the magnitude of the backscattered flux

$$F_{\mathrm{b}}(x, y) = \int_0^{2\pi} \int_{-1}^{0} -\mu I(x, y, s = -1, \mu, \phi)\, \mathrm{d}\mu\, \mathrm{d}\phi. \tag{33}$$

We approximate these integrals using the quadrature rules used to approximate the scattering operator described in Section 3.3.

Plots of some of these results appear in Fig. 2. Here, we have plotted contours of the transmitted and backscattered fluxes normalized to the incident flux on a dB scale defined as $10\log_{10}(F_{\mathrm{t,b}}/F_0)$. These particular computations correspond to a medium of optical thickness $\sigma_{\mathrm{t}}L = 5$ with $\sigma_{\mathrm{s}} = 0.99$, $\sigma_{\mathrm{a}} = 0.01$, and $g = 0.2$. Figs. 2(a) and (b) are plots of computations involving a normally incident $\mu_0 = 1$ and $\phi_0 = 0$ beam of width $\sigma_{\mathrm{t}}w_0 = 1$. Figs. 2(c) and (d) are plots of the same computations, but with an obliquely incident $\mu_0 = 0.7660$ ($\theta_0 = 40°$) and $\phi_0 = 0$ beam of width $\sigma_{\mathrm{t}}w_0 = 1$. Both of these computations used 33 Chebyshev modes, 256 Fourier modes for y, 129 Fourier modes for x (recall that only half of the spectrum is needed since I is real), 10 μ-abscissas, and 8 ϕ-abscissas. As an initial test to verify the accuracy of the method with these parameters, we computed a similar case in which $\sigma_{\mathrm{a}} = 0$ so that power is conserved [2]. With these parameters this method conserves power to within 0.01%.

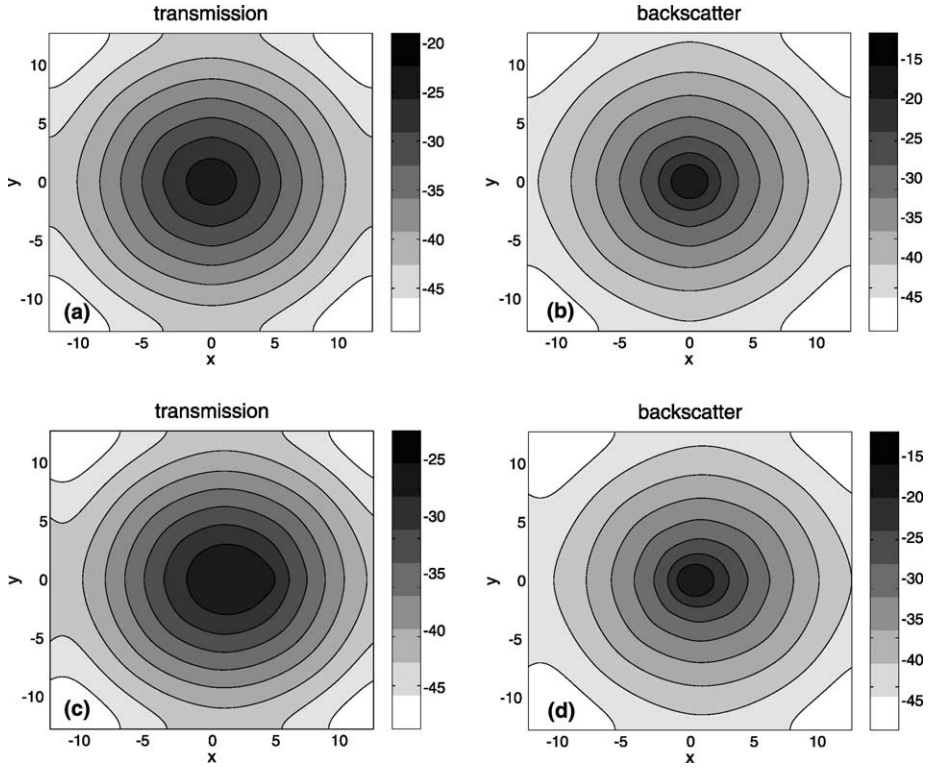

Fig. 2. Example radiative transfer computations. (a) and (b) show, respectively, the contour plots of the transmitted and backscattered flux responses (dB scale) of a normally incident beam ($\mu_0 = 1$) from a homogeneous medium of optical thickness $L = 5$ using the Henyey–Greenstein phase function with $g = 0.2$. The width of the beam, in optical units, is 1. Plots (c) and (d) show a similar computation but for an obliquely incident beam with $\mu_0 = 0.7660$ ($\theta = 40°$) and $\phi = 0$.

In Figs. 2(a) and (b), we clearly observe the radial symmetry in the transmitted and backscattered fluxes manifested from the cylindrically symmetric computation. One particularly advantageous aspect of this method is that one can consider obliquely incident beams. In that case, one simply changes the values of the indices (l', m') in (29) to correspond to the desired direction of incidence. Figs. 2(c) and (d) show an example involving an obliquely incident beam wave. Notice here that the radial symmetry of the transmitted and backscattered fluxes is broken as a result of the oblique incidence.

To ensure that this method is consistent, we compare results computed by this spectral method with those from Monte Carlo simulations. Monte Carlo simulations involve tracing individual photons as they propagate in and interact with the medium, and recording a score each time a photon encounters the scoring region. The scoring method we have used is a ring detector technique that is valid for normally incidence beams ($\mu_0 = 1$). Because this problem is symmetric the ring detector estimates the average flux on a ring rather than the flux at the surface of a *real* detector. Since the score converges to the expected value at the rate const./$\sqrt{N}$, where N is the number of scores, the ring detector technique gives lower variance estimates. Particularly important is the fact that the ring detector has finite variance even in a scattering medium. For a more detailed discussion on Monte Carlo methods for photon transport problems we refer to [9] and references therein.

In Fig. 3 we plot a comparison between results from the spectral method and Monte Carlo simulations. The medium properties are $\sigma_s = 1.0$ and $\sigma_a = 0.0$ with isotropic scattering $g = 0$. The parameters used for the spectral computation are the same as stated above corresponding to Fig. 2 for the normally incident

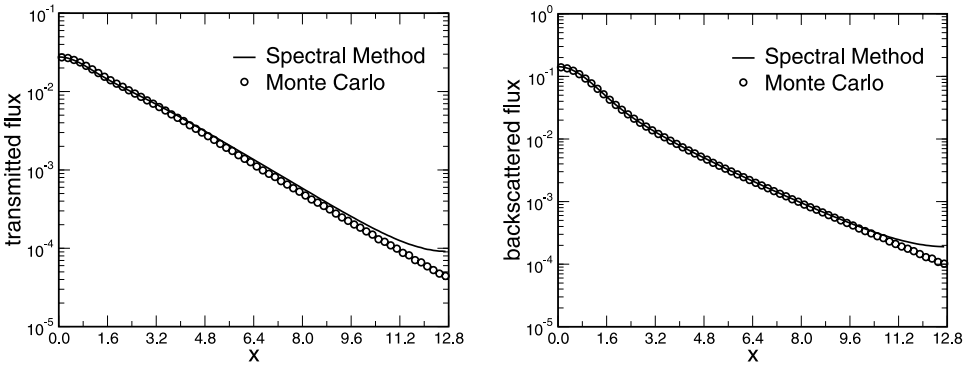

Fig. 3. Comparison between the spectral method (solid line) and a Monte Carlo method. We show the cross-section $y = 0$. The parameters used are the same as in Figs. 2(a) and (b) but with $\sigma_s = 1.0$, $\sigma_a = 0.0$, and $g = 0$.

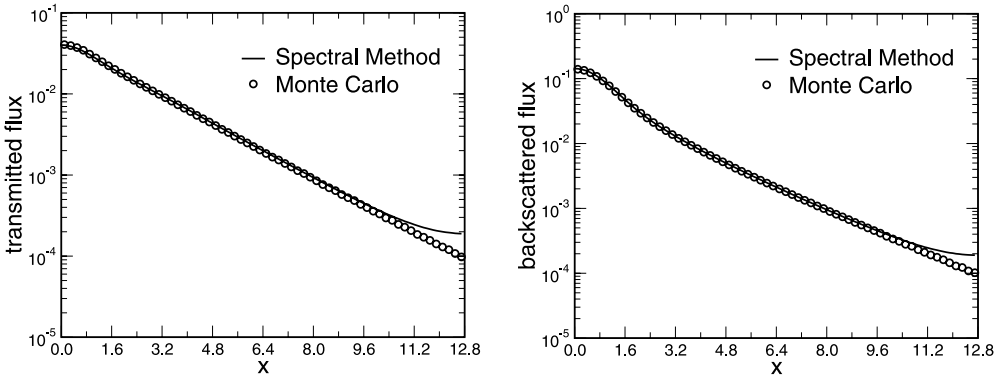

Fig. 4. Same as Fig. 3 but with $g = 0.4$.

beam. Here, we plot the cross-section of the transmitted and backscattered fluxes at $y = 0$ for $x \geqslant 0$. Deviations occurring at large distances from beam center are due to the periodic "wrap-around" in discrete Fourier transform approximations. These errors can be overcome by considering wider spatial domains. Nonetheless, we observe excellent agreement between the two methods thereby demonstrating the consistency of the spectral method.

We plot another comparison in Fig. 4 to examine anisotropic scattering with $g = 0.4$. To account for the higher anisotropy in these computations, we used 10 μ-abscissas and 10 ϕ-abscissas. Otherwise, the parameters settings used for these results are the same as described for examples above. With this particular parameter setting, we obtain power conservation within 0.2%. We still observe excellent agreement between the two different methods apart from the same deviations seen in Fig. 3 at large distances from beam center.

5. Conclusions

We have presented a numerical method for the searchlight problem in which a narrow optical beam impinges a plane-parallel scattering medium. It is not restricted to normal incidence or isotropic scattering. It uses Fourier spectral methods to obtain a one-dimensional equation of transfer for each transverse spatial frequency pair. A Chebyshev spectral approximation for the remaining spatial variable yields a

linear system of integral equations. We use a Clenshaw–Curtis quadrature rule for the polar variable and an extended trapezoid rule for the azimuthal variable to solve these integral equations. We have shown its consistency through comparisons with Monte Carlo simulations of the same problem. With its high accuracy, and relative ease of implementation, this spectral method holds great potential for large scale radiative transfer computations.

References

[1] S. Chandrasekhar, Radiative Transfer, Dover, New York, 1960.
[2] A. Ishimaru, Wave Propagation and Scattering in Random Media, IEEE Press, New York, 1996.
[3] H.-W. Chang, A. Ishimaru, Beam wave propagation and scattering in random media based on the radiative transfer theory, J. Wave–Material Interact. 2 (1987) 41–69.
[4] B.D. Ganapol, D.E. Kornreich, J.A. Dahl, D.W. Nigg, S.N. Jahshan, C.A. Wemple, The searchlight problem for neutrons in a semi-infinite medium, Nucl. Sci. Eng. 118 (1994) 38–53.
[5] L.B. Barichello, C.E. Siewert, The searchlight problem for radiative transfer in a finite slab, J. Comput. Phys. 157 (2000) 707–726.
[6] M.M.R. Williams, Diffusion length and criticality problems in two- and three-dimensional one-speed neutron transport theory. II. Circular cylindrical coordinates, J. Math. Phys. 9 (1968) 1885.
[7] A.D. Kim, A. Ishimaru, Chebyshev spectral method for radiative transfer equations applied to electromagnetic wave propagation and scattering in a discrete random medium, J. Comput. Phys. 152 (1999) 264–280.
[8] A.D. Kim, M. Moscoso, Chebyshev spectral methods for radiative transfer, SIAM J. Sci. Comput. 23 (2002) 2075–2095.
[9] M. Moscoso, J.B. Keller, G. Papanicolaou, Depolarization and blurring of optical images by biological tissue, J. Opt. Soc. Am. A 18 (2001) 948–960.
[10] L.M. Delves, J.L. Mohamed, Computational Methods for Integral Equation, Cambridge University Press, Cambridge, 1985.
[11] T.F. Chan, D.C. Resasco, Generalized deflated block-elimination, SIAM J. Numer. Anal. 23 (1986) 913–924.